Research paper

Circulating extracellular vesicles are endowed with enhanced procoagulant activity in SARS-CoV-2 infection

Carolina Balbi[a,b,1], Jacopo Burrello[c,1], Sara Bolis[a,c,1], Edoardo Lazzarini[c], Vanessa Biemmi[c], Enea Pianezzi[d], Alessio Burrello[e], Elena Caporali[f], Lorenzo Gauthier Grazioli[g], Gladys Martinetti[d], Tanja Fusi-Schmidhauser[g], Giuseppe Vassalli[a,b,h], Giorgia Melli[h,i,2], Lucio Barile[c,h,j,2,*]

[a] Laboratory of Cellular and Molecular Cardiology, Istituto Cardiocentro Ticino, Ente Ospedaliero Cantonale, Lugano, Switzerland
[b] Center for Molecular Cardiology, Zurich, Switzerland
[c] Laboratory for Cardiovascular Theranostics, Istituto Cardiocentro Ticino, Ente Ospedaliero Cantonale Lugano, Switzerland
[d] Laboratory of Microbiology, Ente Ospedaliero Cantonale, Bellinzona, Switzerland
[e] Department of Electrical, Electronic and Information Engineering (DEI), University of Bologna, Bologna, Italy
[f] Cardiology Department, Istituto Cardiocentro Ticino, Ente Ospedaliero Cantonale, Lugano, Switzerland
[g] Internal Medicine Department, Ospedale Regionale di Lugano, Ente Ospedaliero Cantonale, Lugano, Switzerland
[h] Faculty of Biomedical Sciences, Università della Svizzera italiana, Lugano, Switzerland
[i] Laboratory for Biomedical Neurosciences, Neurocenter of Southern Switzerland, Lugano, Switzerland
[j] Institute of Life Science, Scuola Superiore Sant'Anna, Pisa, Italy

ARTICLE INFO

ABSTRACT

Background: Coronavirus-2 (SARS-CoV-2) infection causes an acute respiratory syndrome accompanied by multi-organ damage that implicates a prothrombotic state leading to widespread microvascular clots. The causes of such coagulation abnormalities are unknown. The receptor tissue factor, also known as CD142, is often associated with cell-released extracellular vesicles (EV). In this study, we aimed to characterize surface antigens profile of circulating EV in COVID-19 patients and their potential implication as procoagulant agents.

Methods: We analyzed serum-derived EV from 67 participants who underwent nasopharyngeal swabs molecular test for suspected SARS-CoV-2 infection (34 positives and 33 negatives) and from 16 healthy controls (HC), as referral. A sub-analysis was performed on subjects who developed pneumonia (*n* = 28). Serum-derived EV were characterized for their surface antigen profile and tested for their procoagulant activity. A validation experiment was performed pre-treating EV with anti-CD142 antibody or with recombinant FVIIa. Serum TNF-α levels were measured by ELISA.

Findings: Profiling of EV antigens revealed a surface marker signature that defines circulating EV in COVID-19. A combination of seven surface molecules (CD49e, CD209, CD86, CD133/1, CD69, CD142, and CD20) clustered COVID (+) versus COVID (-) patients and HC. CD142 showed the highest discriminating performance at both multivariate models and ROC curve analysis. Noteworthy, we found that CD142 exposed onto surface of EV was biologically active. CD142 activity was higher in COVID (+) patients and correlated with TNF-α serum levels.

Interpretation: In SARS-CoV-2 infection the systemic inflammatory response results in cell-release of substantial amounts of procoagulant EV that may act as clotting initiation agents, contributing to disease severity.

Funding: Cardiocentro Ticino Institute, Ente ospedaliero Cantonale, Lugano-Switzerland.

1. Introduction

Patients with SARS-CoV-2 infection (COVID-19) experience an abnormal coagulation state. Disseminated intravascular coagulation (DIC) characterized by markedly elevated d-dimer and fibrin degradation products has been reported to develop in about 70% of

* Corresponding author at: Istituto Cardiocentro Ticino, Ente Ospedaliero Cantonale, Via Tesserete 48, 6900 Lugano, Switzerland.
E-mail addresses: lucio.barile@cardiocentro.org, lucio.barile@usi.ch (L. Barile).
[1] These Authors contributed equally to the study.
[2] These authors have contributed equally to this work as senior authors.

Research in Context

Evidence before this study

The outbreak of coronavirus disease 2019 (COVID-19) represents a serious international public health emergency. By January 2021, it accounts for more than 90 millions of cases and about 2 millions of deaths. Coronavirus 2 (SARS-CoV-2) shows tropism for nasopharyngeal and alveolar epithelial cells as well as endothelial cells, all expressing the human counter-receptor angiotensin-converting enzyme 2 (ACE2). The infection causes a severe acute respiratory syndrome accompanied by a systemic inflammatory response that may lead to multi-organ damage and failure. The latter event often implicates thrombotic complications such as widespread venous and arterial microvascular clots. Although increasing evidence shows that COVID-19 patients present a hypercoagulable state, there is no clear explanation for the trigger of such coagulation abnormalities. Several studies have shown that tissue factor (CD142), one of the initiator of the coagulation process in the setting of severe infections, is often associated with cell-released extracellular vesicles (EV). In the present study, we aimed at exploring the role of CD142-bearing EV in COVID-19 patients.

Added value of this study

This is the first antigenic profiling of circulating EV in COVID-19 patients. The analysis revealed a specific surface signature that defines circulating EV in COVID-19. By combining the expression level of seven surface molecules (CD49e, CD209, CD69, CD142, and CD20), we were able to distinguish subjects who tested positive for SARS-CoV-2 on nasopharyngeal swab test, from those who experienced infection symptoms but had a negative test. For certain selected EV markers, this was also true in analog inflammatory status (diagnosis of pneumonia): EV from patients with pneumonia and confirmed diagnosis of SARS-CoV-2 infection were different from those with pneumonia but negative at swab test.

CD142, also known as platelet tissue factor (TF) as it enables the extrinsic pathway of blood coagulation cascade, was one of the most expressed EV surface marker in SARS-CoV-2 positive patients as compared to negative ones. Most important, the CD142 exposed onto surface of EV displayed biological activity, thus suggesting a potential role for EV as a clotting initiation agent in SARS-CoV-2 infection.

Implications of all available evidence

Substantial amounts of inflammatory EV circulate in blood of patients with COVID-19 infection. Circulating EV may act as an effector of coagulation abnormalities that contribute to SARS-CoV-2 severity. This aspect may offer a novel and completely unexplored therapeutic approach, aiming at targeting procoagulant EV in patients. Moreover, our pilot study indicates that EV surface profiling is a potential prognostic biomarker with high clinical impact. Indeed, the level of expression of CD142 directly correlated with hospitalization days and inversely with the count of white blood cells, which is considered one of the indicators of poor prognosis in COVID-19 patients. If validated in a larger cohort of patients, EV specific signature represents an unprecedented biomarker tool that copes with the unmet need of relevant biomarker suitable to identify patients that develop an uncontrolled systemic reaction to SARS-CoV-2 infection.

COVID-19 patients with poor prognosis [1−3]. Abnormal levels of d-dimer were also found in a group of patients managed with standard doses of prophylactic anticoagulant, although characterized by a very low rate of DIC (2%) [4]. Coagulation abnormalities in SAR-CoV-2 patients were also confirmed by recent autopsy studies demonstrating the presence of fibrin deposition and thrombi formation within vessels and capillaries [5].

Derangement of coagulation process often acts as a consequence of systemic inflammatory reaction, leading to unbalancing between coagulation and physiological anticoagulant pathways [6,7]. Several inflammatory mediators, including tumor necrosis factor (TNF)−α, interleukin (IL)−1, and IL−6, act by increasing the expression of tissue factor (TF), also known as CD142, present in sub-endothelial tissue and leukocytes [8,9]. CD142 is generally accepted as the pivotal initiator of the coagulation process in the setting of severe infections [10]. It binds and activates factor VII, leading to the formation of tissue factor-VIIa complexes, which can activate clotting factors X and IX. Landmark studies have shown that TF is expressed on cell surface mainly in a low procoagulant state and it is generally referred to as the "cryptic" TF [11]. It requires an activation ("decryption") step by the redox environment through the oxidoreductase activity of protein disulfide isomerase (PDI), to exert its full procoagulant potential [11−13]. Several studies have shown that CD142 is often associated to circulating microparticles and cell-released extracellular vesicles (EV) [14,15]. EV are well-known players of intercellular crosstalk [16,17] with critical physiological functions in developing and propagating of inflammatory status and infections [18−21]. Indeed EV derived from dendritic cells express on their surface pathogen-derived antigens or cross-reactive antigens that prompt immune responses [22−24]. Similarly, EV released during the development of lung inflammation and injury mediate signal transfer among lung cells and initiate innate immune response [25]. Procoagulant activity of EV is known since 1967 [26], and it has been recently shown in isolated EV from cancer patients' plasma [27,28]. Very recently, Holnthoner et al. showed that TNFα-stimulate endothelial cells to release CD142-bearing vesicles that exert procoagulant activity in fresh whole blood from healthy volunteers [29].

We hypothesized that the cytokine storm occurring in COVID-19 patients might influence surface phenotype of circulating EV. We profiled multiple inflammatory-related antigens, including CD142 expression, onto surface of serum-derived EV and their procoagulant activity in patients who tested positive at SARS-CoV-2 nasopharyngeal swab. We also performed a sub-analysis of EV surface profile and EV procoagulant activity in both group of patients COVID (+) versus COVID (-) who developed pneumonia.

2. Methods

2.1. Ethics

The study was approved by the Ethical Committee of the Ticino Canton, Switzerland (2020-00795, Rif CE TI 3616). Subjects gave informed consent according to the Declaration of Helsinki.

2.2. Data source and collection

Serum samples were collected after the diagnostic work-up from Ente Ospedaliero Cantonale and Istituto Cardiocentro Ticino. They were part of a serum bank of Ente Ospedaliero Cantonale at Laboratory of Microbiology EOLAB, Bellinzona, Switzerland.

The study population consisted of 83 subjects. Sixty-seven with respiratory symptoms (dyspnea, cough, cold) including 28 hospitalized patients diagnosed with pneumonia, were enrolled between March 1, 2020 and May 1, 2020. Symptomatic subjects underwent a molecular test (Polymerase Chain Reaction, PCR), by nasopharyngeal swab for suspected SARS-CoV-2 infection. Sixteen samples were

included from age- and sex-matched healthy controls (HC) from previous studies using the same material, stored at same conditions for the same type of assay.

Exclusion criteria were: (1) Concomitant acute non-respiratory infections; (2) Cancer (active or recent history); (3) Autoimmune or chronic inflammatory diseases; (4) Trauma, bone fractures, hemorrhagic disorders. Patients were grouped according to the result of the nasopharyngeal swab for SARS-CoV-2 infection: 33 patients were negative, COVID (-), and 34 positive, COVID (+), which corresponded to a study power of 90% considering the estimated variability for median fluorescence value of EV surface antigens (2-tails tests for independent samples, Cohen's d coefficient equal to 0.94, and α-error equal to 0.05). Study power estimation was performed by G*Power 3.1. Unblinded investigators recruited patients but were not involved in experimental analysis.

2.3. Blood sample handling

Serial peripheral venous blood samples were collected from subjects at the time of nasopharyngeal swab test. 8.5 ml of blood was collected for each donor, in serum separator tubes (BD Vacutainer SST II, Advance, 8.5 ml) and stored 30 min at room temperature (RT). After clot formation a first centrifugation at 1600 g for 10 min at 4 °C was performed to separate serum from cellular components. Serum was transferred in a new clean tube and centrifuged at 3000 g for 20 min (Fig. 1a). Supernatant was transferred in new clean tube and 10,000 g for 15 min, to remove intact cells, cellular debris and larger EV, and then stored at −80 °C [32].

2.4. Flow-cytometry analysis

Pre-cleared serum samples underwent bead−based EV immunocapture and were analysed by flow cytometer (FC) using MACSPlex human Exosome Kit (Miltenyi; Bergisch Gladbach, Germany; Fig. 1a). Briefly, serum supernatant was incubated with 37 fluorescently labelled capture bead populations, each coated with a specific antibody binding the respective surface epitope, and 2 control bead populations, followed by the EV *detection reagent* (i.e. fluorescently labelled antibodies for CD9/CD63/CD81). Median fluorescence intensity (MFI) was measured on a MACSQuant−Analyzer−10 flow cytometer (Miltenyi) according to previous validation studies [33,34]. All markers were analyzed simultaneously. Surface epitope levels were referenced to EV−specific epitopes by subtracting the respective fluorescence values of blank control from MFI values for individual epitopes and normalizing them for CD9/CD63/CD81 MFI, reflecting EV concentration (Tables S1 and S2). Normalized MFI was reported as nMFI (%).

2.5. Extracellular vesicles isolation

Pre-cleared serum samples (100 μl/donor) underwent over-night centrifugation at 100,000 g using ultracentrifuge Optima XPN and rotor 90 Ti (all from Beckman Coulter). Particle concentrations were determined by dynamic light scattering using NTA technology (Nanosight, Malvern), as previously described (Fig. S1a) [35].

2.6. Tissue factor activity assay

CD142 (tissue factor) activity on intact EV ($1*10^9$ particles) were measured using human Tissue Factor Activity Assay (abcam 108906), as per manufacturer's instructions.

The tissue factor activity assay protocol measures amidolytic activity of the TF/FVIIa complex to activate factor X (FX) to factor Xa. The amount of produced FXa is quantified in absorbance (405 nm) by the release of specific substrate. Blocking experiments were performed pretreating EV with Anti-CD142 antibody at concentration of 15 μg/ml (BioLegend 365206).

2.7. CD142 − FVIIa affinity assay

CD142 (Miltenyi − 130-115-683) and CD63 (Biolegend − 353004) MFI on isolated EV ($1*10^8$ particles) was analyzed by Flow Cytometry as previously described [36]. Samples were pre-incubated with 25nM of recombinant human FVIIa (abcam 108906) or PBS for 30 minutes at 37 degrees. Samples were then acquired with CytoFLEX (Beckman Coulter) and analysis performed with Kaluza (Beckman Coulter).

2.8. TNF-α ELISA assay

Serum level of TNF-α were evaluated using human TNF-α ELISA assay (abcam 181421), as per manufacturer's instructions.

2.9. Western blot

Total proteins were extracted by lysing samples with ice-cold RIPA buffer supplemented with SIGMAFAST^{TM} Protease Inhibitors and Phosphatase Inhibitor Cocktail 3 and 2 (all from Sigma, St. Louis, MI, USA). Protein concentration was determined using BCA (Thermo Fisher Scientific). Proteins were boiled with Laemmli SDS sample buffer 6x (VWR International, Dietikon, Switzerland), separated on 4−20% Mini-PROTEAN®TGX^{TM} Precast Gel, and transferred onto a PVDF membrane with a semi-dry transfer system (all from Bio-Rad Europe, Basel, Switzerland). Membranes were incubated with appropriate antibodies (TF-CD142 ab252918; CD81 ab109201; Syntenin-1 ab19903; TSG101 ab125011; Apo-B48 ab20737; Apo-A1 ab33470 all from abcam) and then with IRDye® 680RD or 800CW goat anti-mouse or goat anti-rabbit secondary Ab (LI-COR Biosciences, Lincoln, Nebraska, USA). Infrared signal was detected using Odyssey CLx Detection System (LI-COR Biosciences). Full images of membranes are provided in Fig. S1b.

2.10. Statistics

Variable distribution was assessed by Kolmogorov−Smirnov test. Normally distributed variables were expressed as mean ± standard deviation and analyzed by T-student test for independent samples or by ANOVA-one way and Bonferroni post-hoc test. Non normally distributed variables were expressed as median [interquartile range] and analyzed by Mann-Whitney test or Kruskal-Wallis test, as appropriated. Categorical variables were expressed as absolute number (percentage) and analyzed by Chi square test (or Fisher test, when appropriated). P of less than 0.05 were considered significant. Correlations were evaluated by Spearman's Rho test. Multivariate logistic regression analysis was performed to evaluate EV surface antigen association with SARS-CoV-2 infection after correction for possible confounding factors. Odds ratio (ORs) were evaluated together with their 95% confidence intervals; an OR greater than 1 indicates an increased likelihood of infection by SARS-CoV-2, and an OR less than 1 a decreased likelihood. Receiver Characteristics Operating (ROC) curves were drawn to estimate the area under the curve (AUC) of EV surface antigens (considered individually or as a compound marker obtained by linear combination of all the others). Youden's J index (J = sensitivity + specificity -1) was calculated to assess the cut-off with the highest accuracy for each EV marker.

Prediction performance of EV specific signature was evaluated by unsupervised learning algorithms. K-means was performed to classify patients in clusters according to EV surface antigen expression. Principal component analysis was used to reduce high-dimensional data into a two-dimensional plot and visualize patient clustering according to SARS-CoV-2 infection.
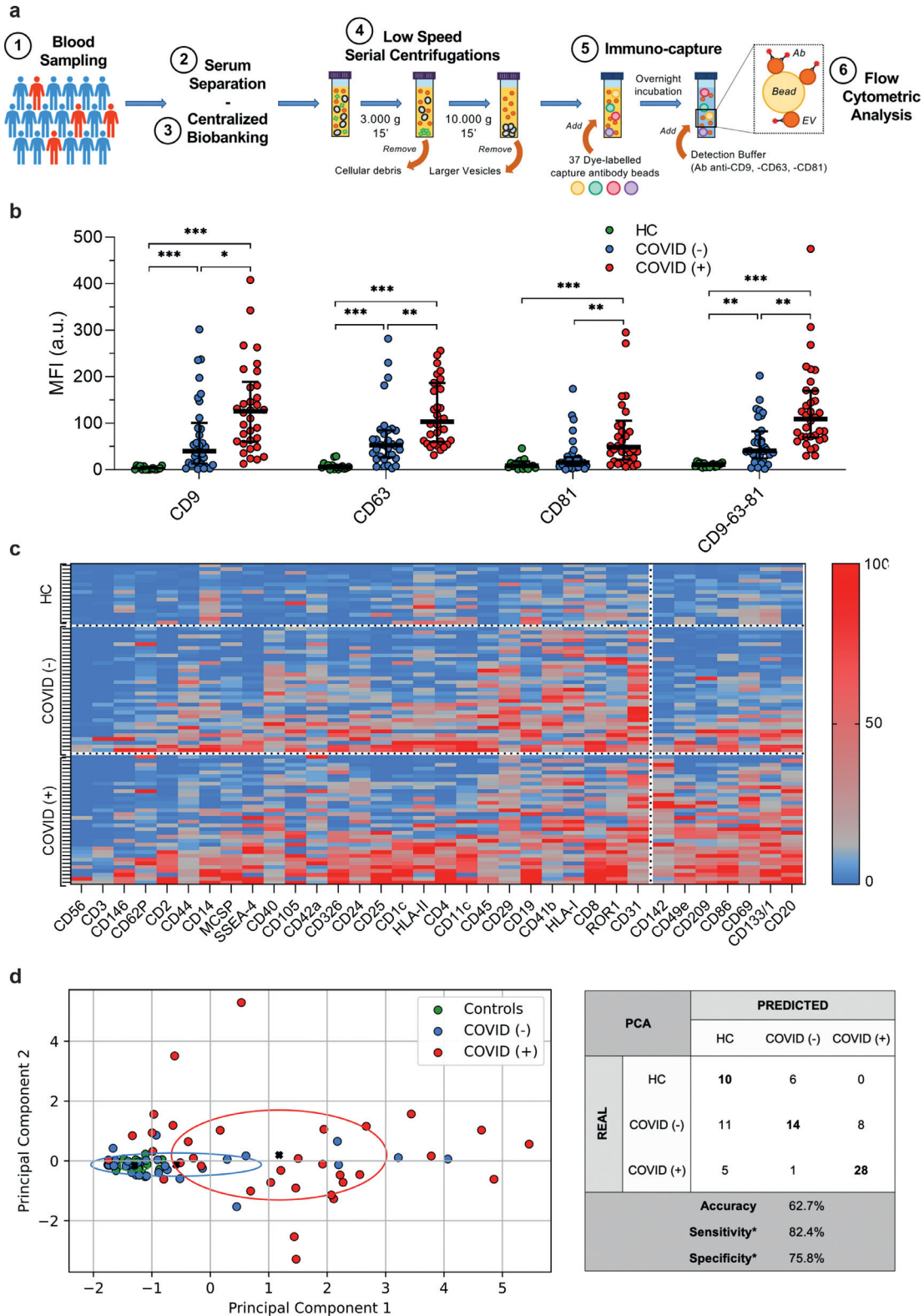
Fig. 1. Profiling of EV surface antigens

The molecular signature derived by EV surface antigen expression allowed the discrimination of patients with or without infection by SARS-CoV-2 ($n = 67$) compared to healthy controls (HC; $n = 16$). (**a**) Schematic illustration of the protocol. (**b**) Median fluorescence intensity (MFI, expressed as arbitrary unit, a.u.) for CD9, CD63, CD81 and for the mean of CD9-CD63-CD81. Dot plots show median and interquartile range; levels of MFI were compared by Kruskal–Wallis test; *$P < 0.05$; **$P < 0.01$; ***$P < 0.001$ (statistics is reported in Supplementary Table S1-S2). (**c**) Heat map showing MFI after normalization by the average MFI of CD9-CD63-CD81 (nMFI; %) for EV surface antigens evaluated by flow cytometry. Blue/red = low/high fluorescence. (**d**) Principal component analysis displaying patient clustering according to EV antigen expression (CD49e, CD209, CD86, CD133/1, CD69, CD142, CD20) and diagnosis of SARS-CoV-2 infection. Each patient is indicated by a point and diagnoses are represented by color (HC, green; COVID [-], blue; COVID [+], red). The principal components 1 and 2 are calculated by weighted linear combinations of the 7 EV markers differentially expressed in patients with or without SARS-CoV-2 infection. The ellipses include patients which falls within the mean +/- SD (principal components 1 and 2 +/- SD). Confusion matrix reports real and predicted diagnosis, accuracy, sensitivity and specificity; *sensitivity and specificity were calculated considering COVID (+) patients vs. COVID (-) and HC grouped together.

Table 1
Demographic parameters.

Variable	HC [n = 16]	COVID (-) [n = 33]	COVID (+) [n = 34]	Overall P-value	Pairwise Comparison		
					C vs. (-)	C vs. (+)	(-) vs. (+)
Age (years)	59 ± 12.0	65 ± 24.8	61 ± 17.4	0.508	–	–	–
Sex (Male; %)	8 (50.0)	17 (51.5)	19 (55.9)	0.905	–	–	–
BMI (Kg/sqm)	25.4 ± 5.84	24.3 ± 4.63	26.6 ± 4.77	0.301	–	–	–
Pneumonia (%)	–	12 (36.4)	16 (47.1)	–	–	–	0.375
Bilat Pneumonia (%)	–	3 (9.1)	10 (29.4)	–	-	–	**0.035**

Demographic characteristics of patients included in the study (n = 83). Normally distributed variables (age, BMI) are expressed as mean ± standard deviation and were analyzed by ANOVA-one way and Bonferroni post-hoc test; categorical variables (sex, pneumonia, bilateral pneumonia) are expressed as absolute number (percentage) and analyzed by Chi square test (or Fisher test, when appropriated); a $P < 0.05$ was considered significant and shown in bold. Bilat, Bilateral.

Analyses and figures were obtained by using IBM SPSS Statistics 26 (IBM, New York, USA), Python 3.5 (library, scikit-learn), and GraphPad PRISM 8.0 (La Jolla, California).

2.11. Role of funding source

Funders had no role in study design, data collection, data analyses, interpretation, or writing of report.

3. Results

3.1. Patients' characteristics

We analyzed serum samples collected from 83 participants. Sixty-seven symptomatic subjects underwent nasopharyngeal swab test for suspected SARS-CoV-2 infection, and were divided in two groups based on the test results: 33 resulted negative for the presence of the virus, COVID (-), while 34 were positive, COVID (+). Sixteen samples were included as referral from age- and sex-matched healthy control (HC) subjects (Table 1). Overall, the mean age was 62 ± 19.9 years and 53.0% were males. Among symptomatic subjects, 12 of 33 (36.4%) and 16 of 34 (47.1%) were diagnosed with pneumonia, in COVID (-) and COVID (+) groups respectively. Pneumonia was bilateral in 29.4% of patients with infection by SARS-CoV-2, and 9.1% negative for the virus ($P = 0.035$).

Several clinical and biochemical parameters were monitored at time of hospitalization for patients with diagnosis of pneumonia with or without SARS-CoV-2 infection ($n = 28$; Table 2). COVID (+) patients displayed lower levels of white blood cells, neutrophils, and monocytes ($P < 0.05$), as compared with COVID (-). No other differences were found in medical history (smoking habit, presence of chronic obstructive pulmonary disease, coronary artery disease, chronic heart failure, hypertension, diabetes, chronic kidney disease), arterial blood gas analysis, and other biochemical parameters ($P > 0.05$ for all comparisons). Among hospitalized patients with upper tract respiratory symptoms, there has been a trend toward a worse outcome in COVID (+) vs. COVID (-) subjects, with a longer duration of hospitalization (median days 14 vs. 8) and a higher incidence of orotracheal intubation, or death (56.3% vs. 33.3%, and 12.5% vs. 0.0%, respectively).

3.2. EV-surface antigens expression differs between groups

We have previously shown that the median fluorescence intensity (MFI) detected by flow cytometer for specific EV surface tetraspanins (CD9, CD63 and CD81) from bio-fluids, can be considered a reliable parameter to evaluate the concentration of circulating vesicles in individuals [19,35,37,38]. CD9/CD63/CD81 MFI as a measure of EV concentration was increased in serum samples from subjects with respiratory symptoms (with or without SARS-CoV-2 infection) compared to HC ($P < 0.001$; Fig. 1b). Notably, the expression levels of tetraspanins significantly increased in EV from COVID (+) as respect to

those derived from serum of COVID (-) subjects. By grouping the surface antigens according to their cellular origin, we found that most of the vesicles have endothelial or platelet origin (Fig. S2). Interestingly, endothelial EV subpopulation showed an increasing trend going from HC to symptomatic patients, with a further increase in COVID (+) patients (Fig. S2).

The median signal intensity for CD9/CD63/CD81 was then used as normalization factor for the MFI of each specific epitope so that positive signals (nMFI) indicate the presence of the respective surface

Table 2
Characteristics of patients with pneumonia

Variable	COVID (-) [n = 12]	COVID (+) [n = 16]	P-value
Age (years)	65 ± 24.9	60 ± 14.1	0.509
Sex (Male; %)	8 (66.7)	11 (68.8)	0.907
BMI (Kg/sqm)	23.8 ± 5.72	26.6 ± 5.24	0.211
Anamnesis			
COPD (%)	2 (16.7)	3 (18.8)	0.887
Smoking habit (%)	0 (0.0)	3 (18.8)	0.112
CAD (%)	3 (25.0)	4 (24.0)	1.000
CHF (%)	2 (16.7)	1 (6.3)	0.378
Hypertension (%)	6 (50.0)	7 (43.8)	0.743
Diabetes (%)	1 (8.3)	4 (25.0)	0.254
CKD (%)	4 (33.3)	4 (25.0)	0.629
Arterial blood gas assay			
pCO2 (KPa)	5.8 ± 1.79	4.6 ± 0.70	0.084
pO2 (KPa)	10.8 ± 1.38	10.2 ± 5.58	0.522
Bicarbonate (mmol/L)	25.9 ± 3.95	23.7 ± 2.87	0.141
Lactic acid (mmol/L)	1.5 [0.6; 1.8]	1.0 [0.7; 1.7]	0.910
Biochemical parameters			
Haemoglobin (g/L)	130 ± 20.6	137 ± 17.5	0.305
WBC (*10E9/L)	9.5 ± 4.39	5.7 ± 2.12	**0.018**
Neutrophils (*10E9/L)	7.6 ± 4.49	4.1 ± 1.86	**0.030**
Lymphocytes (*10E9/L)	0.9 ± 0.61	0.9 ± 0.36	0.730
Monocytes (*10E9/L)	0.58 ± 0.213	0.33 ± 0.174	**0.003**
Eosinophils (*10E9/L)	0.05 ± 0.050	0.05 ± 0.132	0.984
Basophils (*10E9/L)	0.03 ± 0.024	0.03 ± 0.028	0.596
C-reactive protein (mg/L)	17 [9; 105]	49 [14; 122]	0.312
D-dimer (mg/L)	1.02 [0.64; 3.22]	1.09 [0.63; 3.61]	0.906
PT-INR (a.u.)	1.3 [1.1; 1.5]	1.1 [1.0; 1.2]	0.084
aPTT (sec)	31 [27; 37]	33 [30; 36]	0.455
Outcome			
Hospitalization (days)	8 [4; 16]	14 [8; 19]	0.119
Orotracheal intubation (%)	4 (33.3)	9 (56.3)	0.229
Death (%)	0 (0.0)	2 (12.5)	0.204

Characteristic of patients with diagnosis of pneumonia ($n = 28$), with or without infection by SARS-CoV-2. Normally distributed variables (age, BMI, pCO2, pO2, bicarbonate, haemoglobin, WBC) are expressed as mean ± standard deviation and were analyzed by T-student test for independent samples; non normally distributed variables (lactic acid, C-reactive protein, D-dimer, PT-INR, aPTT, hospitalization) are expressed as median [interquartile range] and analyzed by Mann-Whitney test; categorical variables (sex, anamnesis, orotracheal intubation, death) are expressed as absolute number (percentage) and analyzed by Chi square test (or Fisher test, when appropriated); a $P < 0.05$ was considered significant and shown in bold. COPD, Chronic Obstructive Pulmonary Disease; CAD, Coronary Artery Disease; CHF, Chronic Heart Failure (defined as ejection fraction < 35%); CKD, Chronic Kidney Disease (defined as eGFR < 60 mL/min); WBC, White Blood Cells.
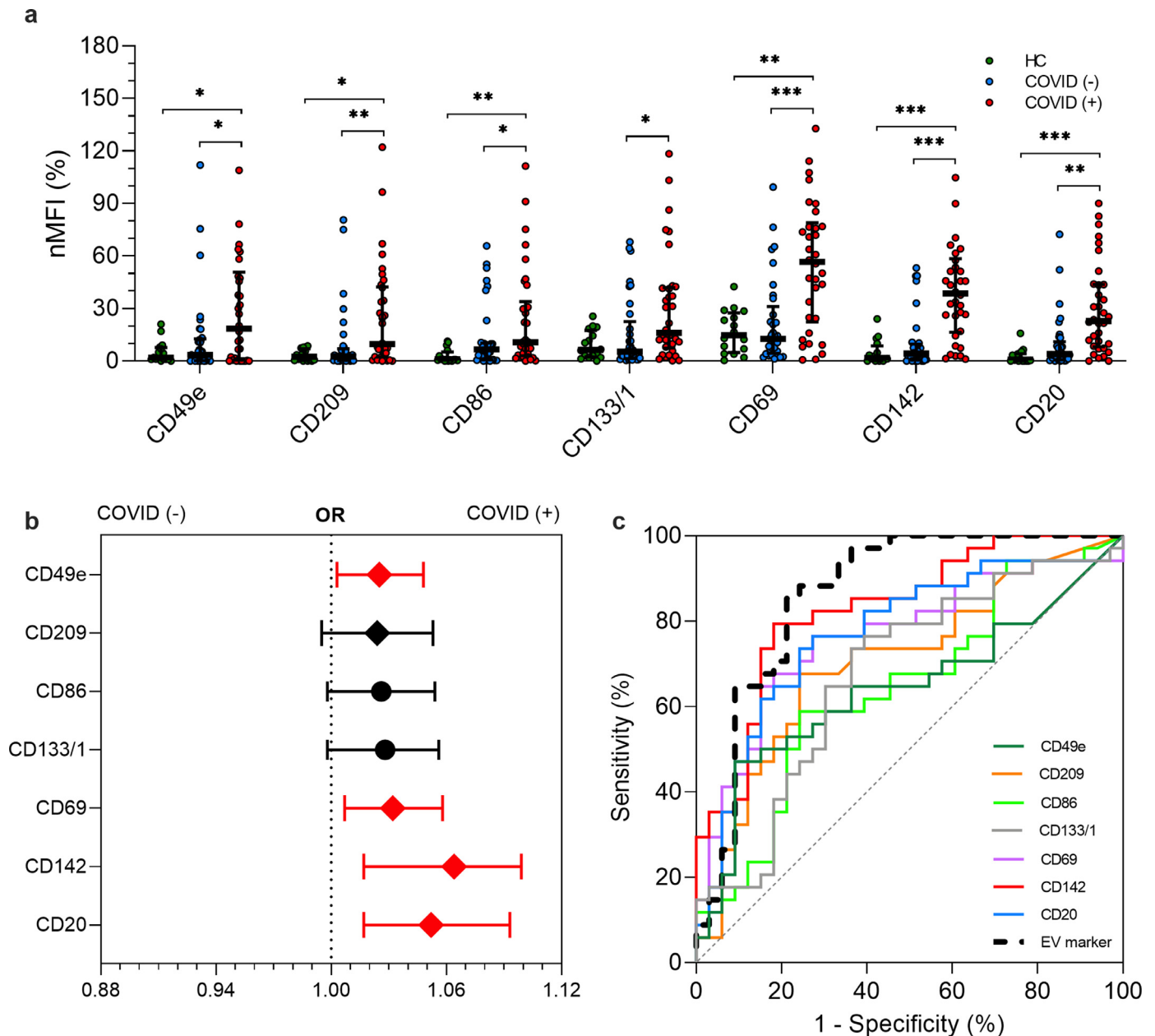
Fig. 2. EV surface antigens associated with infection by SARS-CoV-2

EV surface antigens in patients with or without infection by SARS-CoV-2 (*n* = 67) compared to healthy controls (HC; *n* = 16). Median fluorescence intensity (MFI) was analyzed after normalization by the average MFI of CD9-CD63-CD81 (normalized MFI; nMFI, %). Dot plots show median and interquartile range; levels of MFI were compared by Kruskal−Wallis test; *P < 0.05; **P < 0.01; ***P < 0.001 (statistics is reported in Supplementary Tables S1-4). (**a**) nMFI (%) for the 7 EV surface antigens differentially expressed in patients with or without infection by SARS-CoV-2, compared to HC. (**b**) Association of EV surface antigens with a positive nose-pharyngeal swab after correction for age, sex and diagnosis of pneumonia. Odd ratios (ORs) are shown together with their 95% confidence intervals. Squares were used to indicate significant associations. (**c**) Performance of EV surface antigens in the discrimination of patients COVID [+] vs. COVID [-]. ROC curves are reported for each marker and for a compound EV marker calculated by linear combination of all the others (dashed black line).

epitope within the EV population. Thirteen out of 37 antigens were highly expressed in HC as compared to COVID (-) subjects (Table S1). When comparing COVID (-) and COVID (+) patients 7 EV markers including CD142 (Tissue Factor, TF), CD49e (Integrin α-5), CD209 (Dendritic Cell-Specific Intercellular adhesion molecule-3), CD86 (T-lymphocyte activation antigen), CD69 (Transmembrane C-Type Lectin protein), CD133/1 (prominin-1), and CD20 (β-lymphocyte antigen-20, glycosylated phosphor-protein) were differentially expressed between the two groups (Fig. 2a and Table S1). A heat map reporting expression of vesicles surface profile in individual participants showed a clear clustering in COVID (+) patients for the 7 differentially expressed EV markers (Fig. 1c). None of these seven markers

was significantly different when considering comparison between COVID (-) and HC subjects (Fig. 2a; Table S1), thus showing a characteristic signature that is specific for COVID (+) in spite of overlapping respiratory symptoms.

The EV specific signature resulting from the combination of these antigens by principal component analysis discriminated patients in clusters according to swab test results. Among symptomatic patients, the signature allowed the correct classification of 52 patients out of 67 with a sensitivity 82.4% and specificity of 75.8% (Fig. 1d). Consistently with the expression profile, HC were indistinguishable from COVID (-) group and total accuracy for the three groups was 62.7%.

Four out of seven highly expressed EV markers (CD49e, CD69, CD142, CD20) were significantly associated with SARS-CoV-2 infection as confirmed by multivariate analysis after correction for age, sex, BMI, and diagnosis of pneumonia, as potential confounders (Fig. 2b). Of note CD142 displayed the strongest association with an OR of 1.064 (CI 95% 1.017−1.099 - $P < 0.001$), thus meaning an increase of 6.4% in the likelihood of swab test positivity, per unit of nMFI of this specific marker (Fig. 2b). Interestingly, CD49e, CD86 and CD20 were associated to pneumonia independently from infection by SARS-CoV-2 (Table S3).

Diagnostic performance of each EV marker in discriminating COVID (+) from COVID (-) subjects was assessed by ROC curves analysis (Fig. 2c). The AUC confirmed a reliable performance for all single markers (asymptotical significance with $P < 0.05$ for each curve; Table S4) and ranged from a value of 0.641 for CD49e to a maximum of 0.830 for CD142 (sensitivity 79.4%, specificity 81.8%). Finally, a "compound" EV marker derived by linear combination of the seven differentially expressed epitopes displayed a sensitivity and specificity of 85.3% and 80.8%, respectively with an AUC of 0.865 (95% CI 0.772−0.957 − $P < 0.001$; Fig. 2c).

3.3. EV epitopes in COVID (±) subjects with pneumonia

We evaluated the performance of a specific EV signature in distinguishing patients that were clinically diagnosed as pneumonia due to SARS-CoV-2 infection, from those with pneumonia not related to COVID-19 disease.

As for EV amount among patient with pneumonia, a higher fluorescence levels of CD9, CD63, and CD81 was confirmed in COVID (+) as compared to COVID (-) subjects (Fig. 3a). Among the seven previously identified markers that were differentially expressed between COVID (+) and COVID (-) groups, only two (CD49e and CD209) were not confirmed in the sub-analysis of subjects with pneumonia (Fig. 3b and Table S5). Three out of five EV markers were also significantly associated to SARS-CoV-2 infection at multivariate analysis ($P < 0.05$; CD133/1, CD69, and CD142; Fig. 3c). Once more, after correction for age and sex and BMI the strongest association was found for CD142 (OR 1.103−95% CI 1.017−1.196; $P = 0.017$ Table S6). Finally, the EV signature obtained by linear combination of this five EV markers correctly discriminated 26 of 28 patients according to their diagnosis with an overall accuracy of 92.9% (sensitivity 93.8%, specificity 91.7% - Fig. 3d; pneumonia with or without a demonstrated SARS-CoV-2 infection).

3.4. Functional relevance of EV-tissue factor for COVID19 patients

To assess the biological effect of CD142-bearing EV, vesicles were isolated from serum and the function of CD142 was quantitatively measured by tissue factor activity assay for symptomatic patients ($n = 67$; Table S7). EV from COVID (+) patients showed a 1.9-fold increase in CD142 activity as compared to those with a negative swab ($P < 0.001$; Fig. 4a). Analog trend was observed in COVID (+) versus COVID (-) within the subgroup of patients with pneumonia (2.4-fold increase, $P = 0.020$; Fig. 4a).

Binding of FVII to TF is required for assembly of the functional procoagulant complex (TF-FVIIa) and most of the antibodies against human TF are capable of inhibiting TF activity via blocking the binding of FVII [39,40]. Here, we tested the inhibitory effect on TF activity of the antibody used for its detection and also the hysterical hindrance of FVII for the binding of the fluorescent antibody on the surface of EV. Pre-incubation of EV with the anti-CD142 at same concentration used for the detection assay, induced a reduction in TF activity by 50%, ($P < 0.001$; Fig. 4b). Consistently, pre-treatment of EV with human recombinant FVII, decreased CD142 nMFI by 1.9-times ($P < 0.001$; Fig. 4c). Taken together these data showed the specificity

of assays and suggested a prominent role for CD142 as procoagulant stimulus of EV.

EV derived from patients with diagnosis of pneumonia were further analyzed for the presence of CD142 by WB analysis (Fig. 4d−e). Patients with SARS-CoV-2 infection showed increased CD142-bearing EV levels compared to negative subjects (2-fold increase; $P = 0.009$; Table S7). According to the International Society of Extracellular Vesicles, isolated vesicles tested for CD142 activity were further characterized for the expression of typical EV markers and by nanoparticles tracking analysis (NTA − Fig. S1) [41]. Western blot analysis showed the presence of EV specific luminal markers (TSG101), tetraspanin (CD81), syndecan-binding protein (Syntenin-1) and the absence of apolipoproteins -B48 and -A1 (Fig. 4d). Taken together these results confirmed the presence of EV markers and the absence of relevant contaminants in the samples. Notably, CD142 activity was directly correlated with the expression of CD142 as assessed by both flow cytometry ($R = 0.526$ - $P < 0.001$; Fig. 4g) and western blot analysis ($R = 0.776$ - $P < 0.001$; Fig. 4h).

Because TNF-α has been associated with increased release of CD142-bearing EV by endothelial cells [29], we asked whether the serum level of TNF-α was associated with CD142 activity within COVID (+) patients (Table S8). Interestingly, the TNF-α level in COVID (+) patients displayed a 1.31-fold increase as compared to COVID (-) (12.3 ± 4.17 vs. 9.4 ± 4.85 pg/mL - $P = 0.012$; Fig. 4f). Remarkably, it was directly correlated with the surface expression of CD142 on EV (Rho = 0.243 - $P = 0.048$; Fig. 4i) and with the biological activity of TF carried by EV (Rho = 0.477 - $P < 0.001$; Table S8). A similar trend was found when we focused on patients with a diagnosis of pneumonia. Levels of TNF-α were higher in those with SARS-CoV-2 infection as compared to those who tested negative (1.32-fold increase - $P = 0.029$; Fig. 4f), and directly correlated with EV-carried CD142 activity (Rho = 0.627; $P < 0.001$) and CD142 levels at western blot analysis (CD142-WB; Rho = 0.725 - $P < 0.001$; Fig. 4j).

3.5. Clinical Correlations and patient outcome

Correlations between levels of nMFI for differentially expressed EV markers and clinical/ biochemical parameters were assessed in patients with a diagnosis of pneumonia, with or without SARS-CoV-2 infection (Table 3). Interestingly, mean expression of CD9/CD63/CD81, CD86, CD142, and levels of CD142 at western blot analysis (CD142-WB) were inversely correlated to the number of circulating white blood cells (Rho ranging between −0.373 and −0.480 − $P < 0.05$). A direct correlation was instead found between CD142-WB and aPTT (Rho = 0.590 − $P = 0.010$) or number of hospitalization days (Rho = 0.455 − $P = 0.025$). Finally, levels of CD142-WB were also inversely correlated to arterial blood oxygenation expressed as pO2 (Rho = -0.465; $P = 0.029$). Finally, a sub-analysis evaluating the expression levels of CD142 after stratification for prognosis of patients based on their outcome (a poor outcome was defined in case of orotracheal intubation and/or death) showed that among patients resulted positive for SARSCoV-2, those with poor outcome had significantly higher level CD142 expressed on the surface of circulating EV ($P = 0.013$; Fig. S3).

4. Discussion

We have characterized circulating EV in patients with SARS-CoV-2 infection as compared to subjects with documented absence of the virus at the molecular analysis and to healthy controls as referral group. Circulating EV concentration was increased 2.7-folds in COVID (+) patients at the time of nasopharyngeal swab test compared to COVID (-), as shown by the expression levels of EV-specific markers (CD9, CD63, CD81). Secondly, we report for the first time on a systematic analysis of surface antigen expression by circulating EV in COVID-19 patients, using a multiplex standardized flow cytometric assay
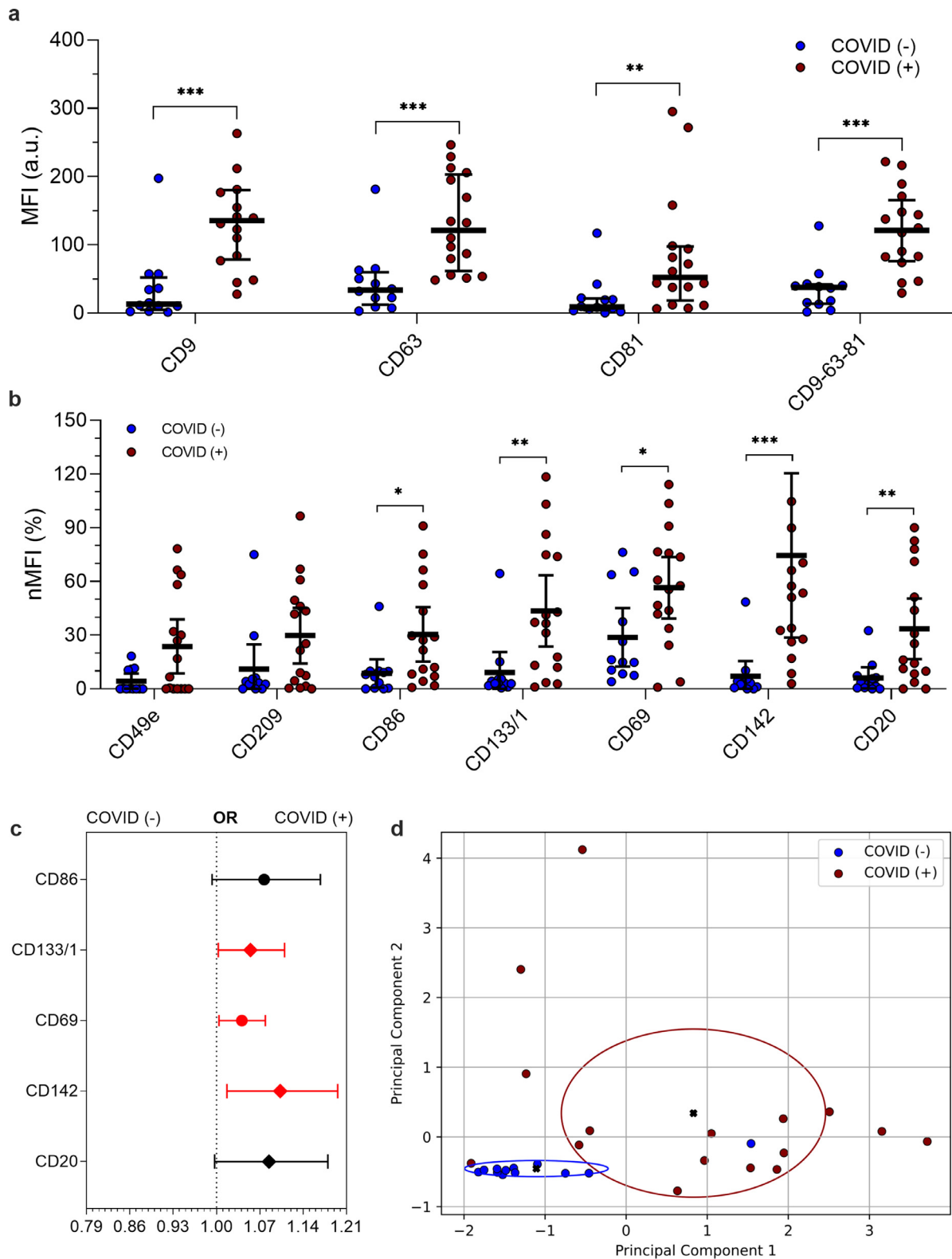
Fig. 3. EV surface antigens associated to pneumonia by SARS-CoV-2

EV surface antigens in patients diagnosed as pneumonia, with or without infection by SARS-CoV-2 (n = 28). Median fluorescence intensity (MFI) was analyzed after normalization by the average MFI of CD9-CD63-CD81 for each patient (normalized MFI; nMFI, %). Dot plots show median and interquartile range; levels of MFI were compared by Mann-Whitney test *$P < 0.05$; **$P < 0.01$; ***$P < 0.001$ (statistics is reported in Supplementary Tables S5-6). (**a**) MFI (arbitrary unit, a.u.) for CD9, CD63, CD81 and for the mean of CD9-CD63-CD81. (**b**) nMFI (%) for the 7 EV surface antigens differentially expressed in patients with or without infection by SARS-CoV-2. (**c**) Association of EV surface antigens with a positive nose-pharyngeal swab after correction for age and sex. Odd ratios (ORs) are showed together with their 95% confidence intervals. Squares were used to indicate significant associations. (**d**) Principal component analysis displaying patient clustering according to EV antigen expression (CD86, CD133/1, CD69, CD142, CD20) and diagnosis of SARS-CoV-2 infection; 26 of 28 patients were correctly classified by the model (accuracy 92.9%).
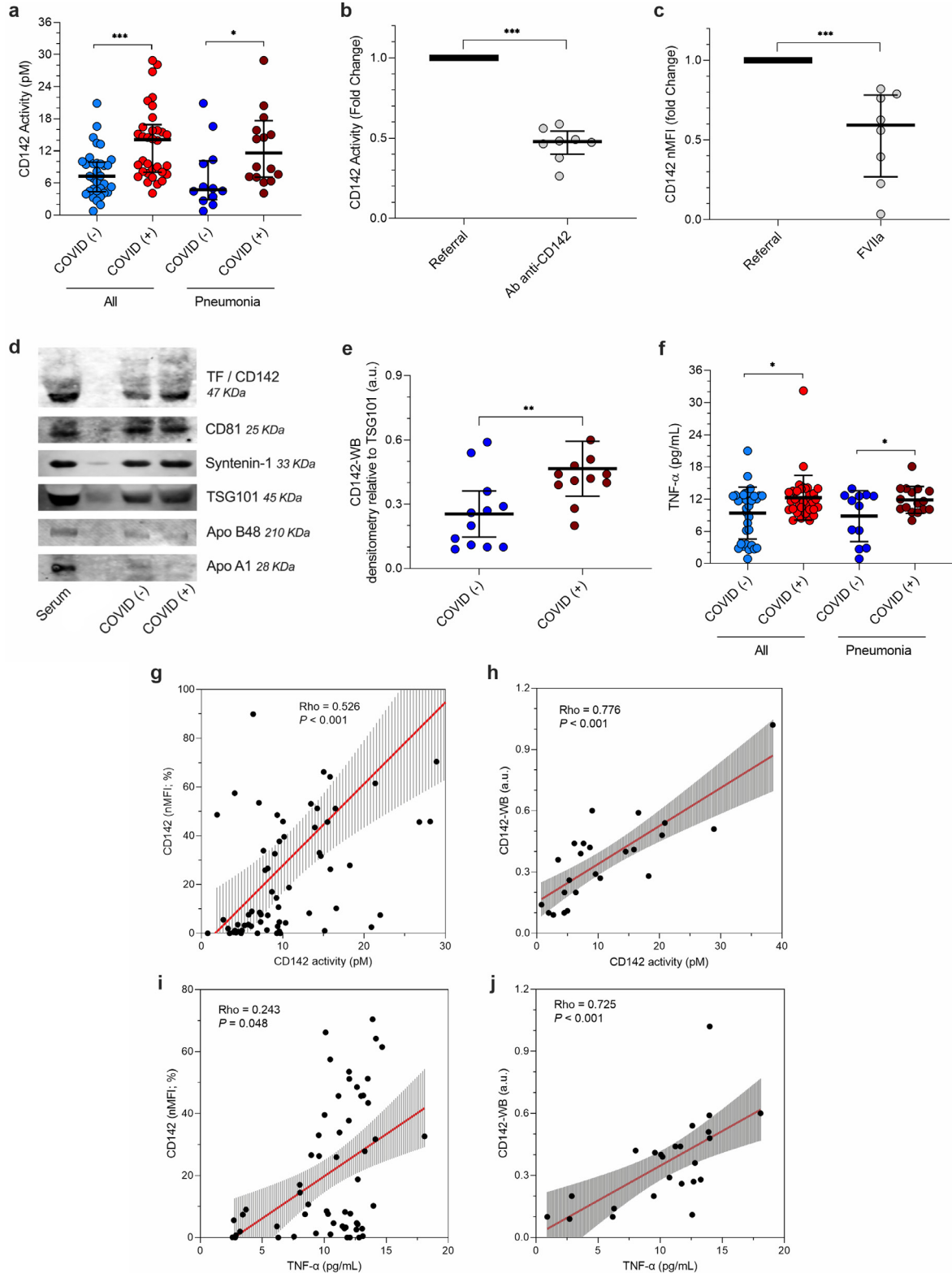
Fig. 4. In-vitro analysis of tissue factor

The activity of extracellular vesicles (EV)- tissue factor (TF) CD142 was evaluated by ELISA in EV obtained from serum samples from patients with or without infection by SARS-CoV-2: all patients (plein boxes; *n* = 67) *vs.* patients with pneumonia (dashed boxes; *n* = 28). CD142 carried by EV was also quantified by western blot. Dot plots show median and interquartile range; CD142 quantification and activity were compared by Mann-Whitney test; levels of TNF-α were compared by T-student test for independent samples; *$P < 0.05$; **$P < 0.01$; ***$P < 0.001$ (statistics is reported in Supplementary Tables S7-8). (**a**) CD142 activity normalized for particle number at NTA (pM per 10^9 particle). (**b**) The specificity of tissue factor activity assay for EV-bearing CD142 was validated by the use of a blocking antibody (anti-CD142); fold change reduction equal to 2.2. (**c**) The specificity of CD142 binding with FVIIa was validated by the pre-treatment with recombinant FVIIa. CD142 nMFI decrease by 1.9 fold compare to untreated EV. (**d**) Representative blots; CD142 is reported together with EV specific markers (CD81, Syntenin-1, TSG101) and potential contaminants (Apolipoprotein -B48, and -A1). (**e**) CD142 quantification by western blot (arbitrary unit, a.u., after normalization for TSG101 expression) in patients diagnosed with pneumonia. (**f**) TNF-α (pg/mL) in serum. (**g**) Correlation between CD142 activity per particle (pM) at tissue factor activity assay and normalized median fluorescence intensity for CD142 (nMFI; %) at flow-cytometric analysis. (**h**) Correlation between CD142 activity per particle (pM) at tissue factor activity assay and CD142 quantification (a.u.) at western blot (CD142-WB) in patients with pneumonia. (**i**) Correlation between mean TNF-α (pg/mL) and CD142 (nMFI; %) at flow-cytometric analysis. (**j**) Correlation between mean TNF-α (pg/mL) and CD142 quantification (a.u.) at western blot (CD142-WB) in patients with pneumonia. Regression lines are reported together with their 95% confidence interval, Spearman's Rho coefficient and level of significance.

Table 3
Correlation of EV parameters with clinical and biochemical patient characteristics

Variable	Age (years)	pO2 (KPa)	Lactic acid (mmol/L)	D-dimer (mg/L)	PT-INR (a.u.)	aPTT (sec)	C-reactive protein (mg/L)	WBC (*10E9/L)	Hosp (days)
CD9-63-81 (MFI)	−0.097	**−0.440**	0.031	−0.134	−0.176	−0.152	0.300	**−0.403**	−0.062
	0.434	**0.015**	0.897	0.595	0.370	0.500	0.096	**0.018**	0.637
CD86 (nMFI; %)	0.180	−0.044	0.201	−0.096	−0.283	0.003	−0.015	**−0.373**	0.179
	0.144	0.816	0.394	0.705	0.144	0.991	0.936	**0.030**	0.167
CD133/1 (nMFI; %)	−0.107	−0.141	−0.030	−0.056	−0.381	0.008	−0.205	−0.338	0.141
	0.389	0.458	0.899	0.826	0.055	0.972	0.260	0.051	0.280
CD69 (nMFI; %)	−0.034	−0.166	0.109	−0.133	−0.272	−0.336	−0.031	−0.222	0.252
	0.788	0.379	0.646	0.598	0.162	0.127	0.866	0.207	0.050
CD20 (nMFI; %)	0.130	−0.118	0.200	−0.039	−0.365	−0.053	−0.141	−0.293	0.082
	0.296	0.533	0.398	0.877	0.056	0.814	0.440	0.093	0.529
CD142 (nMFI; %)	−0.106	−0.086	0.144	0.007	−0.288	−0.006	−0.214	**−0.480**	0.162
	0.393	0.653	0.544	0.977	0.137	0.978	0.240	**0.004**	0.211
CD142-WB (a.u.)	0.128	**−0.465**	0.146	0.042	0.197	**0.590**	0.133	**−0.429**	**0.455**
	0.550	**0.029**	0.634	0.897	0.406	**0.010**	0.546	**0.041**	**0.025**
CD142 activity (pM)	−0.109	−0.219	−0.013	0.039	−0.022	0.225	−0.127	−0.288	0.004
	0.382	0.244	0.957	0.877	0.913	0.315	0.487	0.099	0.976
TNF-α (pg/mL)	−0.180	−0.199	−0.020	−0.054	0.235	0.181	0.154	−0.268	0.052
	0.144	0.293	0.935	0.832	0.228	0.420	0.400	0.125	0.693

Correlations between clinical/biochemical patient characteristics and EV parameters (EV surface antigens differentially expressed in patients diagnosed as pneumonia, with or without infection by SARS-CoV-2; CD142 activity and TNF-α assessed by ELISA; CD142 quantification by WB, CD142-WB; $n = 28$). Correlations are evaluated by Spearman's Rho test. Spearman's Rho coefficient (above) and P-values (below) are reported for each analysis. P-values of less than 0.05 were considered significant and are reported in bold.

that recognizes a panel of 37 EV antigens, mainly involved in inflammation, coagulation process, and endothelial dysfunction. Expression levels of CD49e, CD209, CD69, CD142, and CD20 differed between the two groups and were increased in COVID (+) as compared to COVID (-) patients, independently from age, sex, BMI, and diagnosis of pneumonia, at multivariate analysis. Most important, the EV-surface epitope CD142, which showed the highest discriminating performance at both multivariate models and ROC curve analysis, was biological active, thus suggesting a potential role for EV, as clotting agent in SARS-CoV-2 infection.

EV were initially characterized by their procoagulant activity and described as "platelet dust".[26] However, whether platelets release CD142-bearing EV is controversial and is still unresolved. CD142 is constitutively expressed by sub-endothelial tissue cells, like fibroblasts, perycites [42] and smooth muscle cells [43]. Some authors have indicated the absence of CD142 on/in platelets and challenged the notion that expression of TF (CD142) by activated platelets is a dynamic event [44,45] as others claimed it [46,47]. A broader consensus exist on the fact that inflammatory cytokines can induce endothelial cells to increase expression of CD142 and to sort this protein on the surface of released EV [14,15]. EV of different dimensions, released by endothelial cells upon TNF-α stimulation exert procoagulant activity [29]. Remarkably, the serum levels of TNF-α and IL-6 and IL-8 were significant predictors of disease severity and death in COVID-19 patients [48]. Moreover, TNF-α was significantly elevated in COVID-19 serum compared to healthy donor serum at the time of hospitalization [48]. These findings are in line with our results showing an increased serum level of TNF-α in COVID (+) that significantly correlate with both the expression of CD142 onto surface of EV (assessed by FC and WB analyses), as well as with its procoagulant activity. Such enhanced CD142 activity in EV from serum of COVID-19 patients in comparison to individuals that were negative at the molecular test, was further confirmed even in presence of pneumonia. We speculate that aside from its pathological implication as critical agent promoting viral cell entry in the COVID-19 patients [49], TNF-α may also trigger a massive release of EV by endothelial cells. The sub-analysis assessing the distribution of EV antigens based on cellular origin come in handy of this hypothesis as the endothelial markers are significantly increased in symptomatic patients as compared to healthy controls and further increases in COVID (+) patients. Beside the increased release of vesicles, the endothelium itself may

contribute to enhance the procoagulant activity of TF-bearing circulating particles as injured vessels favors the adhesion of activated platelets that release PDI and contribute to the decryption process [13,30]. Both endothelial injury and platelets activation are common features in COVID-19 disease [31]. SARS-CoV-2 infection was recently associated with an activated (pro-thrombotic) platelet phenotype [31,50]. Canzano et al. provided evidences showing a prominent platelet activation with 10-folds increase in P-selectin (CD62P) in COVID(+) patients as compared to HC [31]. In line with this findings, we found that the CD62P is about five folds more expressed onto EV of symptomatic patients (including COVID(-) and COVID(+)) as compared to HC, but no significant differences were found between symptomatic COVID(+) and COVID(-) subjects. Thus suggesting that although platelets P-selectin is a crucial player for the regulation of the immune response, as it interacts with receptors present on monocytes and neutrophils and enhances TF expression [51], its role is elicited in presence of inflammatory status regardless the specificity of SARS-CoV-2 infection. Zaid and colleagues showed that platelet-derived EV (expressing CD41) were increased in the plasma of COVID-19 patients as compared to healthy subjects. However, the number of circulating platelet vesicles was significantly lower in severe disease as compared to non-severe disease, suggesting that inflammation, rather than thrombosis, might affect production, consumption or sequestration of platelet-derived EV [52].

One limitation of our study is that we do not directly prove that EV contribute to the incidence of venous thromboembolism and/or DIC observed in COVID-19 patients [2,3]. However, we clearly showed that COVID (+) patient-derived EV possess an amidolytic activity by approximately 1.9-fold higher than COVID (-), which increases at 2.4-fold change within subjects with pneumonia. The effect was partially reversed by an anti-CD142 antibody, suggesting a prominent role of TF as procoagulant stimulus of circulating EV. Another limitation of the present study is the low number of included patients. The study has been designed to assess differences between COVID (-) and COVID (+) subjects; the results presented here showed that positivity at swab test for SARS-CoV-2 is associated with different EV phenotype, however it does not allow a conclusive assessment of diagnostic value of the EV surface antigens in COVID-19 patients, as it requires a validation in a larger cohort of patients. Moreover, we cannot define whether this signature is specific for COVID-19 disease, as the large majority of antigens might be theoretical associated with

other acute and chronic inflammatory diseases. In spite of that, a significant correlation was found between levels of CD142 and arterial oxygenation, coagulation parameters, white blood cells' count, and days of hospitalization, all associated with disease severity. Notably, CD142 was significantly more expressed in severe COVID (+) patients undergoing orotracheal intubation and death. This may pave the way for exploring the potential of this specific surface antigen as indicator of disease prognosis in a larger cohort of patients. The reduced number of included patients also limited a wide demographic analysis. The population sex ratio for the study cohort (male(s)/female) was 1.12 that roughly reflect local population distribution; all subject were Caucasian. As for the range of age, 61 ± 17.4 years for COVID (+) patients was compatible with disease-specific age prevalence worldwide [53].

Overall our data suggest an involvement of EV as circulating procoagulant agents and confirm the notion that in a variety of diseases associated with thrombosis, including cancer, CD142-bound EV activity is increased [54,55]. This aspect takes on a wider significance considering that EV possess intrinsically natural properties such as deformable cytoskeleton, 'gel-like' cytoplasm and enrichment in amounts of anionic phospholipids (e.g. phosphoserines) in the outer leaflets of membrane that prevents the self-aggregation, and confer biophysically / structural integrity and resistance to rupture during trafficking in vivo. This may enhance their circulation time and increase the possibility of exerting their procoagulant activity at distance in different body districts [56]. Therefore, we can envision a potential approach aiming to reduce the number of circulating prothrombotic EV [18,57] with the goal to improve patients' outcome in this disease. Such approach may represent mechanistic rationale laying beyond the available evidences of protective effect observed in COVID-19 patients using immunosuppressive therapies such as the TNF-α inhibitors [58-61].

Contributors

C.B., J.B., and S.B., data generation and interpretation, manuscript writing; E.L., V.B., G.V., and G.Me., critical review; A.B.; data interpretation; E.P., E.C., L.G.G., G.Ma. and T.F.S. sample collection; L.B. study design, data interpretation, manuscript writing. All authors read and approved the final version of the manuscript.

Data sharing statement

All data acquired and analyzed during the present study are not publicly available but are available from the corresponding author on reasonable request.

Declaration of Competing Interest

Authors have nothing to disclose.

Acknowledgments

Supplementary materials

Supplementary material associated with this article can be found, in the online version, at doi:10.1016/j.ebiom.2021.103369.

References

[1] Tang N, Li D, Wang X, Sun Z. Abnormal coagulation parameters are associated with poor prognosis in patients with novel coronavirus pneumonia. J Thromb Haemost 2020;18(4):844–7.

[2] Guan WJ, Ni ZY, Hu Y, et al. Clinical characteristics of coronavirus disease 2019 in China. N Engl J Med 2020;382(18):1708–20.

[3] Zhou F, Yu T, Du R, et al. Clinical course and risk factors for mortality of adult inpatients with COVID-19 in Wuhan, China: a retrospective cohort study. Lancet 2020;395(10229):1054–62.

[4] Al-Samkari H, Karp Leaf RS, Dzik WH, et al. COVID-19 and coagulation: bleeding and thrombotic manifestations of SARS-CoV-2 infection. Blood 2020;136(4):489–500.

[5] Fox SE, Akmatbekov A, Harbert JL, Li G, Quincy Brown J, Vander Heide RS. Pulmonary and cardiac pathology in African American patients with COVID-19: an autopsy series from New Orleans. Lancet Respir Med 2020;8(7):681–6.

[6] Levi M. Pathogenesis and diagnosis of disseminated intravascular coagulation. Int J Lab Hematol 2018;40(Suppl 1):15–20.

[7] Bikdeli B, Madhavan MV, Jimenez D, et al. COVID-19 and thrombotic or thromboembolic disease: implications for prevention, antithrombotic therapy, and follow-up: JACC state-of-the-art review. J Am Coll Cardiol 2020;75(23):2950–73.

[8] Nawroth PP, Stern DM. Modulation of endothelial cell hemostatic properties by tumor necrosis factor. J Exp Med 1986;163(3):740–5.

[9] Nawroth PP, Handley DA, Esmon CT, Stern DM. Interleukin 1 induces endothelial cell procoagulant while suppressing cell-surface anticoagulant activity. Proc Natl Acad Sci USA 1986;83(10):3460–4.

[10] van der Poll T. Tissue factor as an initiator of coagulation and inflammation in the lung. Crit Care 2008;12(Suppl 6):S3.

[11] Tomazzolli R, Serra MD, Bellisola G, Colombatti M, Guella G. A fluorescence-based assay for the reductase activity of protein disulfide isomerase. Anal Biochem 2006;350(1):105–12.

[12] Bach RR. Tissue factor encryption. Arterioscler Thromb Vasc Biol 2006;26(3):456–61.

[13] Reinhardt C, von Bruhl ML, Manukyan D, et al. Protein disulfide isomerase acts as an injury response signal that enhances fibrin generation via tissue factor activation. J Clin Investig 2008;118(3):1110–22.

[14] Zwicker JI, Trenor 3rd CC, Furie BC, Furie B. Tissue factor-bearing microparticles and thrombus formation. Arterioscler Thromb Vasc Biol 2011;31(4):728–33.

[15] Dignat-George F, Boulanger CM. The many faces of endothelial microparticles. Arterioscler Thromb Vasc Biol 2011;31(1):27–33.

[16] Barile L, Vassalli G. Exosomes: Therapy delivery tools and biomarkers of diseases. Pharmacol Ther 2017.

[17] Thery C. Exosomes: secreted vesicles and intercellular communications. F1000 Biol Rep; 3: 15.

[18] Biemmi V, Milano G, Ciullo A, et al. Inflammatory extracellular vesicles prompt heart dysfunction via TRL4-dependent NF-kappaB activation. Theranostics 2020;10(6):2773–90.

[19] Vacchi E, Burrello J, Di Silvestre D, et al. Immune profiling of plasma-derived extracellular vesicles identifies Parkinson disease. Neurol Neuroimmunol Neuroinflamm 2020;7(6).

[20] Bachelier K, Biehl S, Schwarz V, et al. Parvovirus B19-induced vascular damage in the heart is associated with elevated circulating endothelial microparticles. PLoS One 2017;12(5):e0176311.

[21] Konadu KA, Chu J, Huang MB, et al. Association of cytokines with exosomes in the plasma of HIV-1-seropositive individuals. J Infect Dis 2015;211(11):1712–6.

[22] Segura E, Nicco C, Lombard B, et al. ICAM-1 on exosomes from mature dendritic cells is critical for efficient naive T-cell priming. Blood 2005;106(1):216–23.

[23] Andre F, Chaput N, Schartz NE, et al. Exosomes as potent cell-free peptide-based vaccine. I. Dendritic cell-derived exosomes transfer functional MHC class I/peptide complexes to dendritic cells. J Immunol 2004;172(4):2126–36.

[24] Gutierrez-Vazquez C, Villarroya-Beltri C, Mittelbrunn M, Sanchez-Madrid F. Transfer of extracellular vesicles during immune cell-cell interactions. Immunol Rev 2013;251(1):125–42.

[25] Lee H, Abston E, Zhang D, Rai A, Jin Y. Extracellular vesicle: an emerging mediator of intercellular crosstalk in lung inflammation and injury. Front Immunol 2018;9:924.

[26] Wolf P. The nature and significance of platelet products in human plasma. Br J Haematol 1967;13(3):269–88.

[27] Hernandez C, Orbe J, Roncal C, et al. Tissue factor expressed by microparticles is associated with mortality but not with thrombosis in cancer patients. Thromb Haemost 2013;110(3):598–608.

[28] Thaler J, Ay C, Weinstabl H, et al. Circulating procoagulant microparticles in cancer patients. Ann Hematol 2011;90(4):447–53.

[29] Holnthoner W, Bonstingl C, Hromada C, et al. Endothelial cell-derived extracellular vesicles size-dependently exert procoagulant activity detected by thromboelastometry. Sci Rep 2017;7(1):3707.

[30] Kiouptsi K, Reinhardt C. Protein disulfide-isomerase - a trigger of tissue factor-dependent thrombosis. Clin Hemorheol Microcirc 2016;64(3):279–86.

[31] Canzano P, Brambilla M, Porro B, et al. Platelet and endothelial activation as potential mechanisms behind the thrombotic complications of COVID-19 patients. JACC Basic Transl Sci 2021.

[32] Pedersen KW, Kierulf B, Neurauter A. Specific and generic isolation of extracellular vesicles with magnetic beads. Methods Mol Biol 2017;1660:65–87.

[33] Koliha N, Wiencek Y, Heider U, et al. A novel multiplex bead-based platform highlights the diversity of extracellular vesicles. J Extracell Vesicles 2016;5:29975.

[34] Wiklander OPB, Bostancioglu RB, Welsh JA, et al. Systematic methodological evaluation of a multiplex bead-based flow cytometry assay for detection of extracellular vesicle surface signatures. Front Immunol 2018;9:1326.

[35] Burrello J, Biemmi V, Dei Cas M, et al. Sphingolipid composition of circulating extracellular vesicles after myocardial ischemia. Sci Rep 2020;10(1):16182.

[36] Balbi C, Bolis S, Vassalli G, Barile L. Flow cytometric analysis of extracellular vesicles from cell-conditioned media. J Vis Exp 2019(144).

[37] Burrello J, Bolis S, Balbi C, et al. An extracellular vesicle epitope profile is associated with acute myocardial infarction. J Cell Mol Med 2020.

[38] Castellani C, Burrello J, Fedrigo M, et al. Circulating extracellular vesicles as non-invasive biomarker of rejection in heart transplant. J Heart Lung Transplant 2020.

[39] Basavaraj MG, Olsen JO, Osterud B, Hansen JB. Differential ability of tissue factor antibody clones on detection of tissue factor in blood cells and microparticles. Thromb Res 2012;130(3):538–46.

[40] Morrissey JH, Fair DS, Edgington TS. Monoclonal antibody analysis of purified and cell-associated tissue factor. Thromb Res 1988;52(3):247–61.

[41] Thery C, Witwer KW, Aikawa E, et al. Minimal information for studies of extracellular vesicles 2018 (MISEV2018): a position statement of the International Society for Extracellular Vesicles and update of the MISEV2014 guidelines. J Extracell Vesicles 2018;7(1):1535750.

[42] Butenas S, Bouchard BA, Brummel-Ziedins KE, Parhami-Seren B, Mann KG. Tissue factor activity in whole blood. Blood 2005;105(7):2764–70.

[43] Drake TA, Morrissey JH, Edgington TS. Selective cellular expression of tissue factor in human tissues. Implications for disorders of hemostasis and thrombosis. Am J Pathol 1989;134(5):1087–97.

[44] Bouchard BA, Mann KG, Butenas S. No evidence for tissue factor on platelets. Blood 2010;116(5):854–5.

[45] Bouchard BA, Krudysz-Amblo J, Butenas S. Platelet tissue factor is not expressed transiently after platelet activation. Blood 2012;119(18):4338–9 ; author reply 9-41.

[46] Camera M, Brambilla M, Toschi V, Tremoli E. Tissue factor expression on platelets is a dynamic event. Blood 2010;116(23):5076–7.

[47] Zillmann A, Luther T, Muller I, et al. Platelet-associated tissue factor contributes to the collagen-triggered activation of blood coagulation. Biochem Biophys Res Commun 2001;281(2):603–9.

[48] Del Valle DM, Kim-Schulze S, Huang HH, et al. An inflammatory cytokine signature predicts COVID-19 severity and survival. Nat Med 2020;26(10):1636–43.

[49] Haga S, Yamamoto N, Nakai-Murakami C, et al. Modulation of TNF-alpha-converting enzyme by the spike protein of SARS-CoV and ACE2 induces TNF-alpha production and facilitates viral entry. Proc Natl Acad Sci USA 2008;105(22):7809–14.

[50] Bongiovanni D, Klug M, Lazareva O, et al. SARS-CoV-2 infection is associated with a pro-thrombotic platelet phenotype. Cell Death Dis 2021;12(1):50.

[51] Maugeri N, Brambilla M, Camera M, et al. Human polymorphonuclear leukocytes produce and express functional tissue factor upon stimulation. J Thromb Haemost 2006;4(6):1323–30.

[52] Zaid Y, Puhm F, Allaeys I, et al. Platelets Can Associate with SARS-Cov-2 RNA and are hyperactivated in COVID-19. Circ Res 2020.

[53] Group WHOREAfC-TW, Sterne JAC, Murthy S, et al. Association between administration of systemic corticosteroids and mortality among critically Ill patients with COVID-19: a meta-analysis. JAMA 2020;324(13):1330–41.

[54] Hisada Y, Mackman N. Measurement of tissue factor activity in extracellular vesicles from human plasma samples. Res Pract Thromb Haemost 2019;3(1):44–8.

[55] Hisada Y, Alexander W, Kasthuri R, et al. Measurement of microparticle tissue factor activity in clinical samples: a summary of two tissue factor-dependent FXa generation assays. Thromb Res 2016;139:90–7.

[56] Wan S, Zhang L, Wang S, et al. Molecular recognition-based DNA nanoassemblies on the surfaces of nanosized exosomes. J Am Chem Soc 2017;139(15):5289–92.

[57] Essandoh K, Yang L, Wang X, et al. Blockade of exosome generation with GW4869 dampens the sepsis-induced inflammation and cardiac dysfunction. Biochim Biophys Acta 2015;1852(11):2362–71.

[58] Valenzuela-Almada MO, Putman MS, Duarte-Garcia A. The protective effect of rheumatic disease agents in COVID-19. Best Pract Res Clin Rheumatol 2021:101659.

[59] Valenti M, Facheris P, Pavia G, et al. Non-complicated evolution of COVID-19 infection in a patient with psoriasis and psoriatic arthritis during treatment with adalimumab. Dermatol Ther 2020;33(4):e13708.

[60] Tursi A, Angarano G, Monno L, et al. COVID-19 infection in Crohn's disease under treatment with adalimumab. Gut 2020;69(7):1364–5.

[61] Kunisaki R, Tsukiji J, Kudo M. Potential inhibition of COVID-19-driven pneumonia by immunosuppressive therapy and anti-TNFalpha antibodies: a case report. J Crohns Colitis 2020.